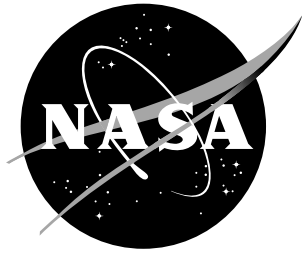


NASA / TM-2001-211051
ARL-TR-2435



Application of a Fiber Optic Distributed Strain Sensor System to Woven E-Glass Composite

*Robert F. Anastasi
U.S. Army Research Laboratory
Vehicle Technology Directorate
Langley Research Center, Hampton, Virginia*

*Craig Lopatin
Langley Research Center, Hampton, Virginia*

August 2001

The NASA STI Program Office ... in Profile

Since its founding, NASA has been dedicated to the advancement of aeronautics and space science. The NASA Scientific and Technical Information (STI) Program Office plays a key part in helping NASA maintain this important role.

The NASA STI Program Office is operated by Langley Research Center, the lead center for NASA's scientific and technical information. The NASA STI Program Office provides access to the NASA STI Database, the largest collection of aeronautical and space science STI in the world. The Program Office is also NASA's institutional mechanism for disseminating the results of its research and development activities. These results are published by NASA in the NASA STI Report Series, which includes the following report types:

- **TECHNICAL PUBLICATION.** Reports of completed research or a major significant phase of research that present the results of NASA programs and include extensive data or theoretical analysis. Includes compilations of significant scientific and technical data and information deemed to be of continuing reference value. NASA counterpart of peer-reviewed formal professional papers, but having less stringent limitations on manuscript length and extent of graphic presentations.
- **TECHNICAL MEMORANDUM.** Scientific and technical findings that are preliminary or of specialized interest, e.g., quick release reports, working papers, and bibliographies that contain minimal annotation. Does not contain extensive analysis.
- **CONTRACTOR REPORT.** Scientific and technical findings by NASA-sponsored contractors and grantees.

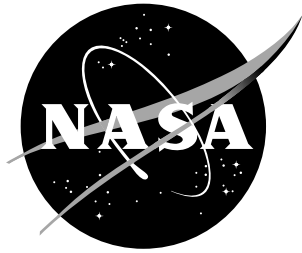
- **CONFERENCE PUBLICATION.** Collected papers from scientific and technical conferences, symposia, seminars, or other meetings sponsored or co-sponsored by NASA.
- **SPECIAL PUBLICATION.** Scientific, technical, or historical information from NASA programs, projects, and missions, often concerned with subjects having substantial public interest.
- **TECHNICAL TRANSLATION.** English-language translations of foreign scientific and technical material pertinent to NASA's mission.

Specialized services that complement the STI Program Office's diverse offerings include creating custom thesauri, building customized databases, organizing and publishing research results ... even providing videos.

For more information about the NASA STI Program Office, see the following:

- Access the NASA STI Program Home Page at <http://www.sti.nasa.gov>
- E-mail your question via the Internet to help@sti.nasa.gov
- Fax your question to the NASA STI Help Desk at (301) 621-0134
- Phone the NASA STI Help Desk at (301) 621-0390
- Write to:
NASA STI Help Desk
NASA Center for AeroSpace Information
7121 Standard Drive
Hanover, MD 21076-1320

NASA / TM-2001-211051
ARL-TR-2435



Application of a Fiber Optic Distributed Strain Sensor System to Woven E-Glass Composite

Robert F. Anastasi
U.S. Army Research Laboratory
Vehicle Technology Directorate
Langley Research Center, Hampton, Virginia

Craig Lopatin
Langley Research Center, Hampton, Virginia

National Aeronautics and
Space Administration

Langley Research Center
Hampton, Virginia 23681-2199

August 2001

The use of trademarks or names of manufacturers in the report is for accurate reporting and does not constitute an official endorsement, either expressed or implied, of such products or manufacturers by the National Aeronautics and Space Administration or the U.S. Army.

Available from:

NASA Center for AeroSpace Information (CASI)
7121 Standard Drive
Hanover, MD 21076-1320
(301) 621-0390

National Technical Information Service (NTIS)
5285 Port Royal Road
Springfield, VA 22161-2171
(703) 605-6000

Application of a Fiber Optic Distributed Strain Sensor System to Woven E-Glass Composite

R.F. Anastasi

U.S. Army Vehicle Technology Directorate, ARL, AMSRL-VT-S, Nondestructive Evaluation Sciences Branch, NASA Langley Research Center, Hampton, VA 23681

C.M. Lopatin

NRC Post-Doctoral Associate, Nondestructive Evaluation Sciences Branch, NASA Langley Research Center, Hampton, VA 23681

Abstract - A distributed strain sensing system utilizing a series of identically written Bragg gratings along an optical fiber is examined for potential application to Composite Armored Vehicle health monitoring. A vacuum assisted resin transfer molding process was used to fabricate a woven fabric E-glass/composite panel with an embedded fiber optic strain sensor. Test samples machined from the panel were mechanically tested in 4-point bending. Experimental results are presented that show the mechanical strain from foil strain gages comparing well to optical strain from the embedded sensors. Also, it was found that the distributed strain along the sample length was consistent with the loading configuration.

INTRODUCTION

Sensors embedded in a composite material can be used to monitor the manufacturing process and for structural health monitoring in critical applications. Although various sensors are available, optical fibers are the predominant choice due to their small size and greatest compatibility with the host material. Three of the most common type of optical fiber sensors are the Intrinsic Fabry-Perot Interferometer, Extrinsic Fabry-Perot Interferometer, and Bragg grating [1]. The most advantageous sensor is the Bragg grating sensor because its simple construction leaves the strength of the optical fiber intact and strain levels can be deduced from optical wavelength shifts. Recently a fiber optic strain sensor system has been developed [2,3] which allows for a series of identical Bragg grating sensors to be written on a long section of optical fiber and be read individually. Each sensor on the optical fiber is read using a system that establishes the location and wavelength (and thus strain) of each grating. With this system about 500 measurement locations on a 8m length of optical fiber can be made with the Bragg grating sensors spaced from 12.7mm to 25.4mm apart. The high density of strain measurements along one optical fiber gives this system potentially high sensor coverage on a structure with minimal weight. This optical strain sensor system has been applied to measuring strain in coupons of tensile-loaded graphite-composites [4] and is being examined for use in the X-33 Re-useable Launch Vehicle [5]. Another potential

application of this optical strain sensor system is for health monitoring of a Composite Armored Vehicle (CAV) which is an advanced technology demonstrator of an all-composite ground combat vehicle. The CAV upper hull is made of a glass/epoxy laminate with embedded ceramic tiles that serve as armor. Multiple distributed strain measurements would help monitor the structural health of such a vehicle and determine damage location and severity. In this paper, we examine the potential application of this optical strain sensor system by manufacturing glass/epoxy composite samples with embedded distributed fiber optic strain sensors and conducting mechanical tests.

FIBER OPTIC SENSORS SYSTEM

A fiber Bragg grating is a periodic modulation of the refractive index in the core of a single mode optical fiber. This modulation is photo-induced by exposing the fiber to an interference pattern between two UV laser beams. By changing the angle between the two beams the modulation of the interference pattern can be controlled. The resulting Bragg sensor reflects a narrow frequency band of light proportional to the periodic modulation. The center frequency reflected is $\lambda = 2n\Lambda$ [6], where n is the index of refraction of the fiber core, and Λ the grating spacing. The strain is then defined as $\varepsilon = (\lambda - \lambda_b)/\lambda_b$, where λ_b is the baseline wavelength. When the strain equation is corrected for material properties, it becomes [5]

$$\varepsilon = K \left(\frac{\lambda - \lambda_b}{\lambda_b} - \xi \Delta T \right) \quad (1)$$

where the constant K is a function of the refractive index, Poisson's ratio, and strain-optic constants of the fiber, ξ is the thermal-optic coefficient, and ΔT is the change in temperature.

The system [2] used to read the multiple Bragg gratings is illustrated in figure 1. This system uses a frequency (or wavelength) swept laser-diode as a light source. Laser-light intensity, reflected from the air gap, reference fiber, and Bragg grating produce an interference that is detected and recorded for post processing. Intensity data processing yields grating location and wavelength or strain. The processing involves computing the amplitude of the Fourier transform of the intensity data and computing the power spectra of individually windowed gratings to obtain grating peak wavelength. The peak wavelength and base wavelength are then used to calculate strain.

COMPOSITE PANEL

A vacuum assisted resin transfer molding process was used to manufacture an E-glass/epoxy composite panel 10-ply thick and approximately 1050.0 x 340.0 x 6.35 mm in size. The material used in the panel was a 24 oz woven fabric and the resin was Dow 411-350 epoxy vinyl ester. In the manufacturing process a length of optical fiber with Bragg grating sensors was placed on the first ply and held in place with a small dot of hot

glue before laying down the second ply. A schematic of the panel, in Figure 2 shows the approximate locations of the optical fibers, the dashed lines, and the grayed areas, the test samples that were cut from the panel. The optical fibers exited the composite lay-up and extended approximately 30 cm from the edge of the panel. These optical fiber extensions were connected to the distributed strain sensor system. The smaller width test samples were initially cut to a width of 5.08 cm and then re-machined to a width of 4.45 cm to fit the 4-point loading fixture. The two larger size test samples were approximately 15.24 cm wide. In process of handling the panel, two of the fiber extensions broke and in the machining process all but three fiber extensions failed. The three remaining test samples (of thinner width) were strain gauged. Two gages were applied, one to the top and one on the bottom, opposite each other along the center of the test sample. Figure 3 shows a strain gage on one side of the coupon and Figure 4 shows an optical fiber exiting the end of the coupon.

TESTING AND MEASUREMENTS

Each sample was tested under a 4-point bend arrangement. The testing arrangement and sample dimensions are illustrated in Figure 5. The supports were spaced 25.4 cm apart and two loading points were spaced 10.16 cm apart. Maximum deflection was limited to the height of the supports on the 4-point loading fixture and was approximately 32 mm. The deflection of a test sample (without strain gages) was 30.5 mm at a load of 510 lbs. During testing, the samples were loaded in 50 lb increments, up to loads of 350 to 500 lbs. At each increment, strain gage output, fiber optic-strain data, and testing machine cross head displacement were recorded. The fiber optic strain sensor was on the roller support side of the test fixture and thus the Bragg gratings were subjected to elongation or tensile loads.

These tests were conducted at room temperature and the duration of each measurement was on the order of a minute. It was therefore assumed that the temperature was constant and could be eliminated from equation (1). The constant K in this equation, a function of the optical fiber, was measured by equating mechanical strain to fiber optic-strain for a single optical fiber sensor, in a separate calibration experiment. This optical fiber sensor was stretched with a micrometer displacement stage while elongation and optical sensor readings were taken. A value of $K=1.45$ was obtained and used to convert fiber optic sensor measurements to strain.

Results

Testing machine cross head displacement and tensile strain gage readings are shown in Figures 6 and 7, respectively, for each sample. A linear range of displacement and strain can be seen in these plots up to approximately 300 lbs. After this load level the displacements and strains are nonlinear. For sample C, composite fiber breaking could be heard at the higher load levels and a slight curvature was evident for each sample when it was removed from the testing machine, thus the test samples yielded. A pre-

yield value for the material modulus was calculated using Euler-Bernoulli beam theory. The modulus value obtained was $E = 26.61 \text{ GPa}$ ($3.86 \times 10^6 \text{ psi}$).

Figure 8 shows the amplitude of the Fourier transform of the raw data for sample A, at 100 lbs. It shows the reflection of 29 Bragg gratings plotted against its location along the optical fiber. The large peak at location 2.81 m is a reflection from the end of the fiber and corresponds approximately to the end of the sample. The Bragg grating width and spacing are 5.0 mm and 15 mm, respectively. An example spectrum of a windowed grating, one unstrained and another strained is shown in Figure 9. The spectrum for the strained grating is not uniform and exhibits a spectrum broadening. At first, we thought that this broadening could in part be due to the rollers pinching the optical fibers. Upon examination, it was found that this broadening occurred only for the gratings between the rollers and not for the ones before or after the strained region. Thus, the pinching was not causing the broadening. It is probable that the optical fiber is most likely being loaded non-uniformly and has a strain distribution across its diameter. This non-uniform loading is due to the loading geometry and causes the induced strain to change as a function of the distance from the center horizontal-axis of the material. This non-uniform strain causes a strain-induced birefringence in the optical fiber that causes the polarized light, injected into the fiber for sensing, to be modulated [7]. Thus, the broadening may in part be due to a non-uniform strain across the diameter of the optical fiber. The results show that this broadening did not inhibit determining the peak wavelength. For the example, the unstrained grating has a peak at a wavelength of 1557.111 nm and the strained grating has a peak wavelength at 1559.812 nm. Using equation (1), the resulting strain for location 2.628 is $2.52 \times 10^{-3} \mu\text{ in/in}$. Similar calculations were used to calculate strain from other Bragg gratings on each of the samples. Figures 10, 11, and 12 compare strain gage readings to a Bragg grating located at approximately the center of the sample. The strain difference for Sample A has a strain variation between mechanical and optical strain of about 2-3%. For Sample B, the strain data initially compares within about 8% and then changes to about 15%. Since the optical strain at the upper loads is parallel to the strain gage reading, it is possible that the optical fiber slipped within the matrix of the composite. Sample C shows a strain variation of about 6% except the last point. An examination of the Bragg grating for this point and load level showed that its reflection was uneven across the width of the sensor and thus true strain readings would be questionable.

Figures 13, 14, and 15 show the optical strain distribution along the length of the sample for load levels of 0, 100, 200, and 300 lbs. For reference, a schematic of the sample and its loading points is positioned in each graph. The position of this schematic is based on the strain distribution and that the strain is zero outside the support points. For example, the bottom supports, in Figure 13, are located at approximately 2.77 m and 2.51 m. This difference is 0.26 m and is approximately equal to 0.25 m, the distance between loading points. The strains across the sample increases with load as expected but are not as smooth as expected. This is may be due, in part, to the weave in the fabric of the composite material producing local strain variations.

The strain at location 2.66 m, in Figure 13 is initially consistent with other gratings around it, but becomes inconsistent at higher loads. Closer examination showed that the width of the reflection became narrower for increasing load, possibly due to a weakness in the optical fiber or local de-bonding of the sensor. Allowing for these variations the strain distributions are consistent with loading.

DISCUSSION

The results illustrate that it is feasible to use distributed strain sensors to measure tensile bending strain in woven glass/epoxy composite material. Mechanical strain measurements compared well with optical strain measurements and strain distributions along the length of the test sample were reasonable. Disagreement between optical and mechanical strain readings may be due in part to placement of the sensor relative to the weave of the composite fabric and that the optical sensor and mechanical strain gage were not identically co-located.

Although the measurement results indicate feasibility, the manufacturing of components with embedded fiber optic sensors requires more attention. The optical fibers exiting the manufactured panel were very fragile and some failed due to handling. Also, the long fiber optic leads exiting the ends of the panel could not be machined to a finished edge because of the optical fiber extensions. Thus ingress and egress of the optical fiber from the composite material is a major problem. Another problem or area of concern is durability of the fiber optic sensors. If the optical sensor slips within the composite matrix then inaccurate strain readings would result. However, losing one or two optical sensors along a long series of sensors may be acceptable. Also of concern is that the system can not measure dynamic strains, as the strain must be held constant for the duration of the laser scan, which typically last a few seconds. However, technology improvements may result in higher laser sweep-speeds and make dynamic measurements possible.

REFERENCES

1. Belk, J.H., J.J. Kelly, and R.M. Crane, "A Summary of DARPA's Embedded Sensors for Submarine Structures Program." ASME Symposium on Adaptive Structures and Material Systems, November 19, 1996.
2. Froggatt, M. and J. More, "Distributed Measurement of Static Strain in an Optical Fiber with Multiple Bragg Gratings at Nominally Equal Wavelength," *Applied Optics*, Vol. 37, No. 10, 1 April 1998.
3. Froggatt, M., "Distributed Measurement of the Complex Modulation of a Photoinduced Bragg Grating in an Optical Fiber," *Applied Optics*, Vol. 35, No. 25, 1 September 1996.

4. Brown, T., K. Wood, B. Childers, R. Cano, B. Jensen, R. Roggowski, "Fiber Optic Sensors for Health Monitoring of Morphing Aircraft," SPIE 6th Annual International Symposium on Smart Structures and Materials, Newport Beach, California, March 1-5, 1999.
5. Melvin, L. et.al., "Integrated Vehicle Health Monitoring (IVHM) for Aerospace Vehicles," International Workshop on Structural Health Monitoring, Stanford CA, 18-20 September 1997.
6. Kersey A.D., M/A. Davis, H.J. Patrick, M. LeBlanc, K.P. Koo, C.G. Askins, M.A. Putnam, and E.J. Friebele, "Fiber Grating Sensors," Journal of Lightwave Technology, Vol. 15, No. 8, August 1997.
7. Krohn, D.A., "Fiber Optic Sensors Fundamentals and Applications," Instrument Society of America, Research Triangle Park, NC, 1992.

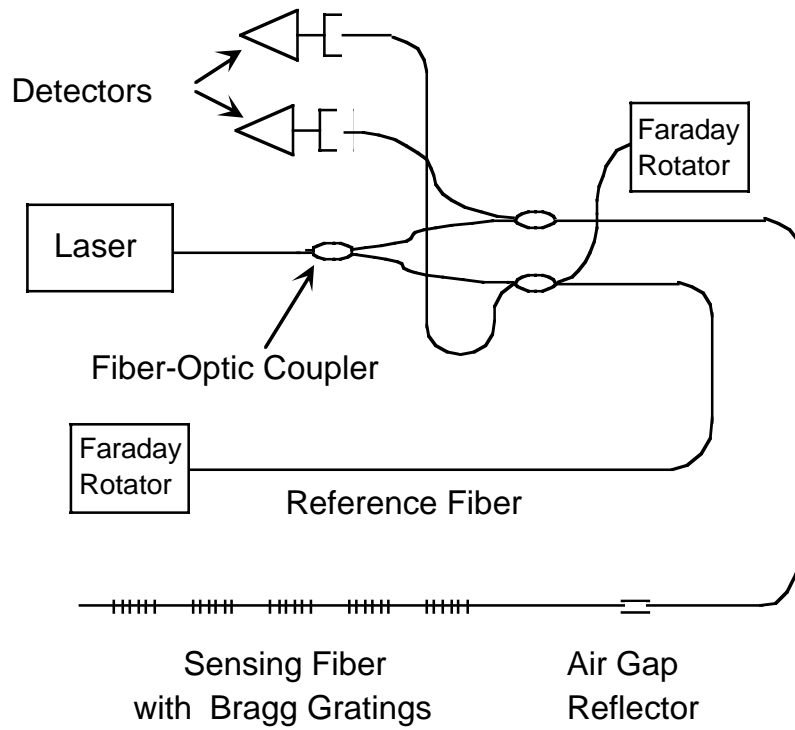


Figure 1. Schematic of distributed Bragg-grating strain sensing system

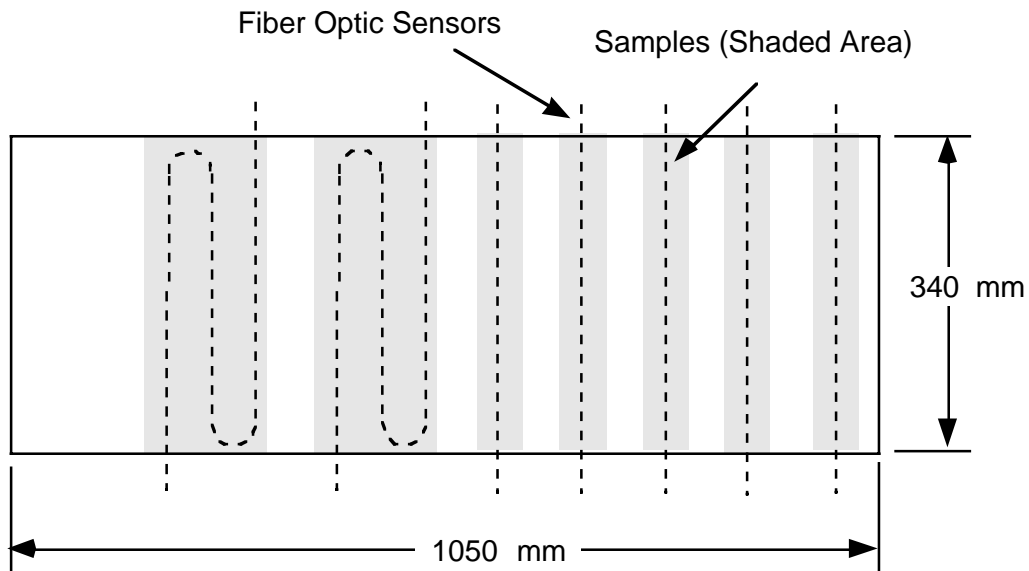


Figure 2. Layout of E-glass composite panel with embedded optical fiber sensors. Panel thickness is 10 ply and approximately 6.35mm. Dashed lines are the position of the optical fibers located in the thickness direction between the 1st and 2nd ply.

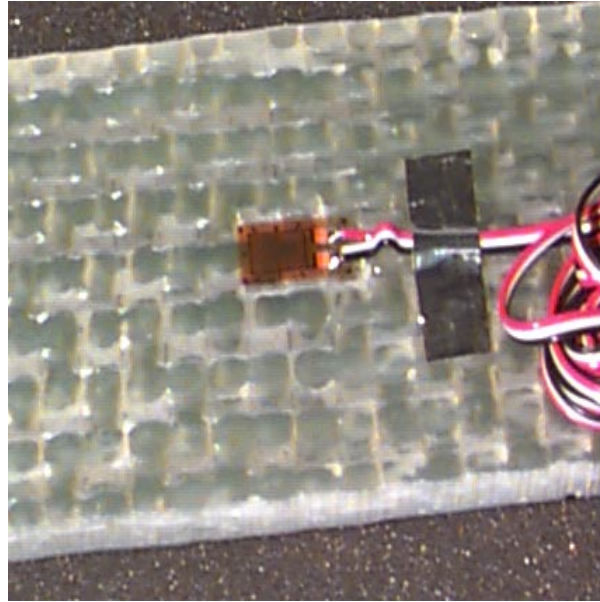


Figure 3. Close up of embedded sensor panel with attached 6.35mm (1/4 inch), 350 Ohm strain gage.

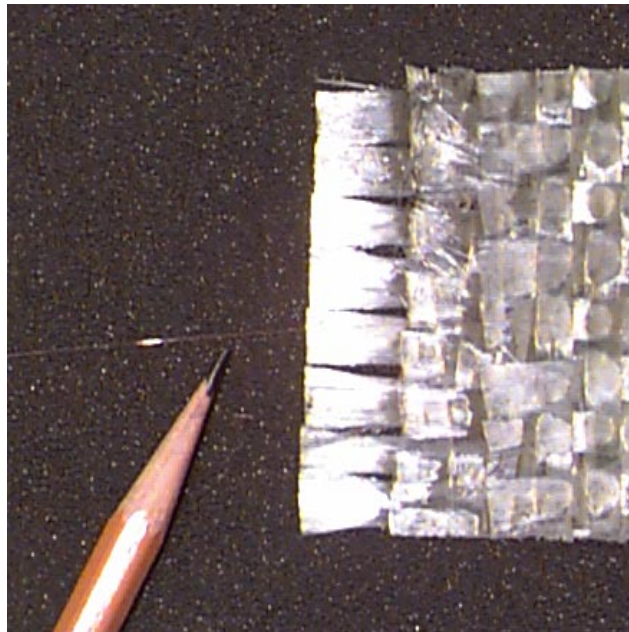


Figure 4. Close up at end of sample showing the fiber optic egression from the sample. The pencil is pointing to the fiber optic sensor.

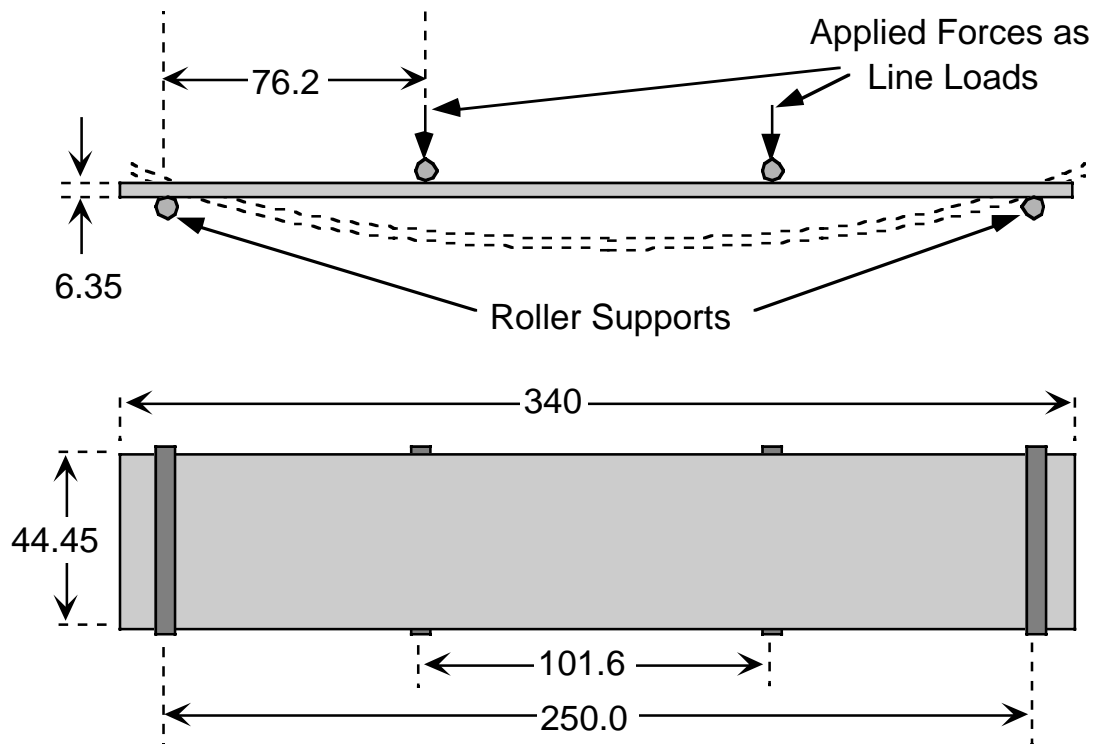


Figure 5. Four-point loading arrangement and sample dimensions. Dimensions are in mm.

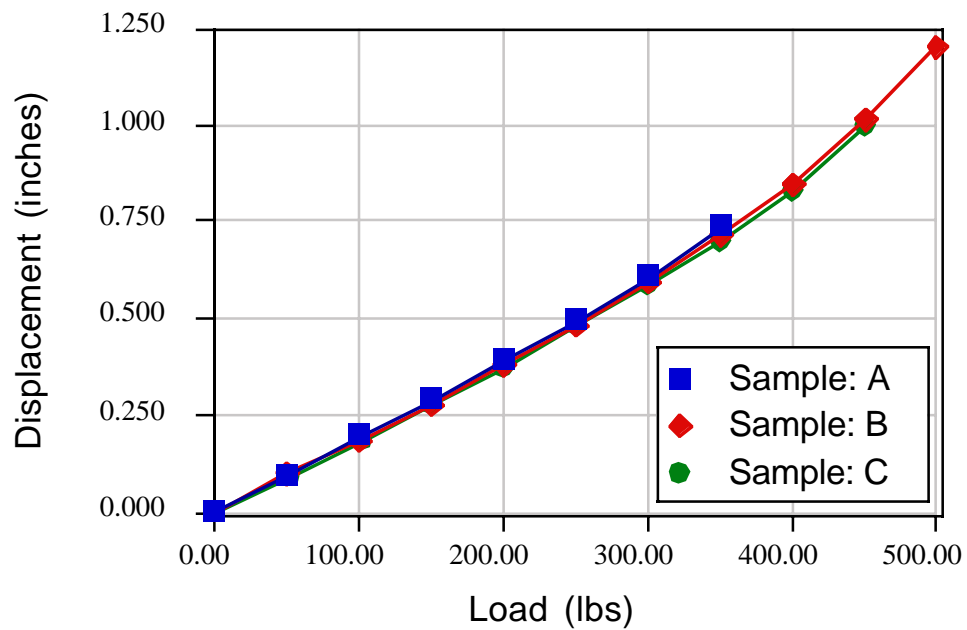


Figure 6. Applied load versus testing machine cross head displacement for Samples A, B, and C. Displacements in the downward direction are shown as positive values.

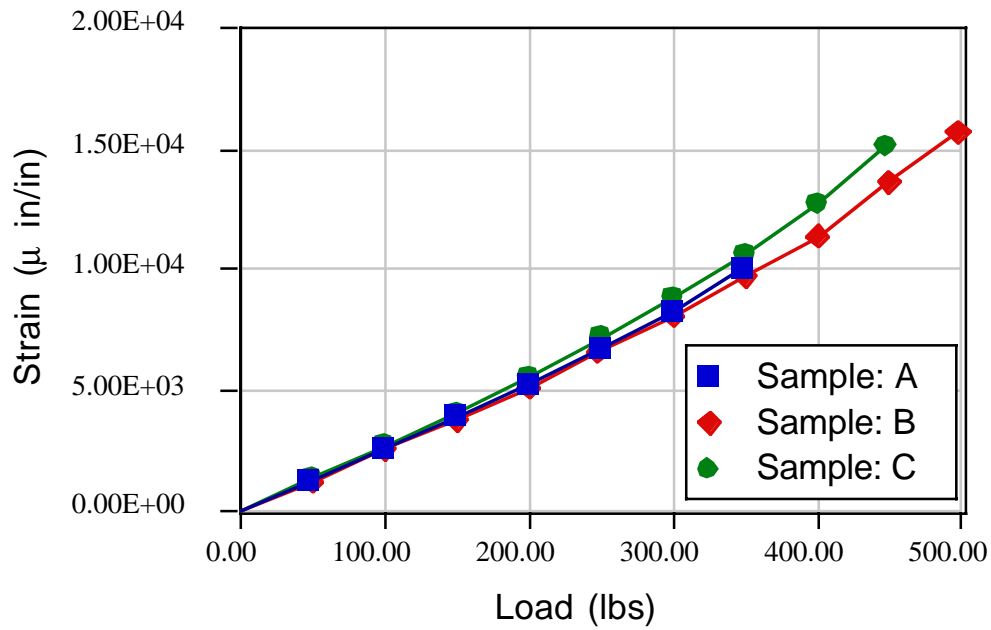


Figure 7. Applied load versus bottom or tensile strain gage reading for Samples A, B, and C.

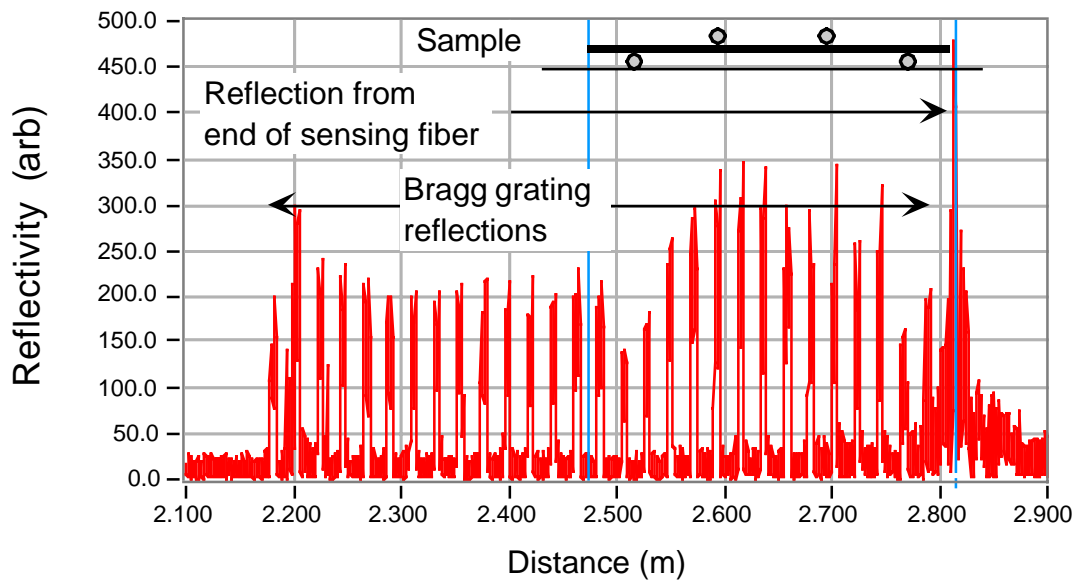


Figure 8. Reflections in the sensing fiber, for Sample A, showing the Bragg grating reflections, reflection from the end of the sensing fiber, and approximate location of sample.

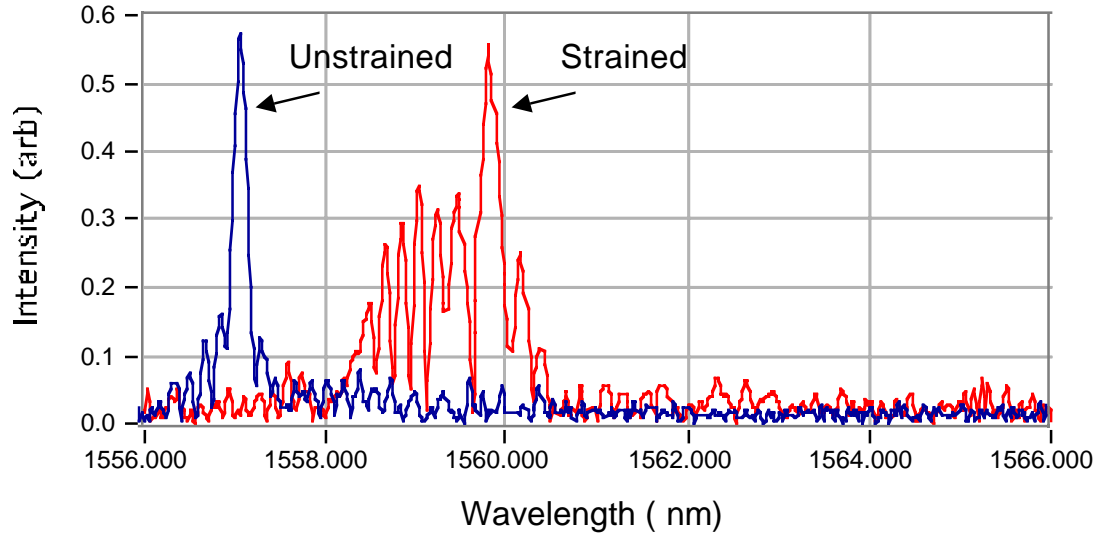


Figure 9. Fourier-transform of the Bragg grating reflection that is located outside the sample and approximately at the center of Sample A for a 100 lb load. Peak amplitude is at wavelength 1557.111 nm and 1559.812 nm respectively.

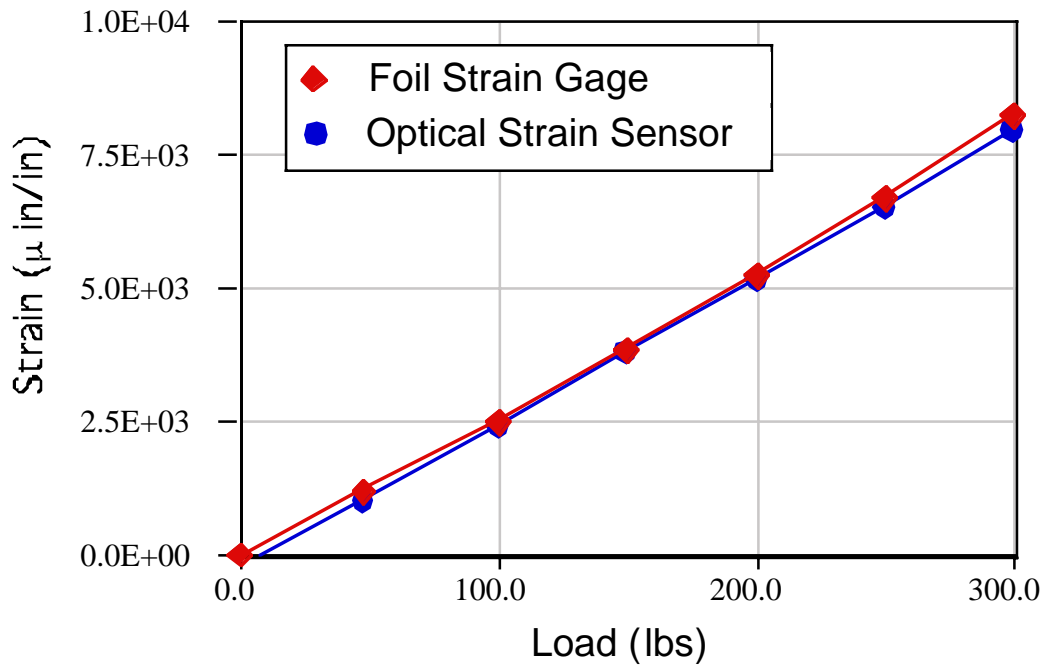


Figure 10. Sample A, comparison of foil strain gage and optical strain sensor data

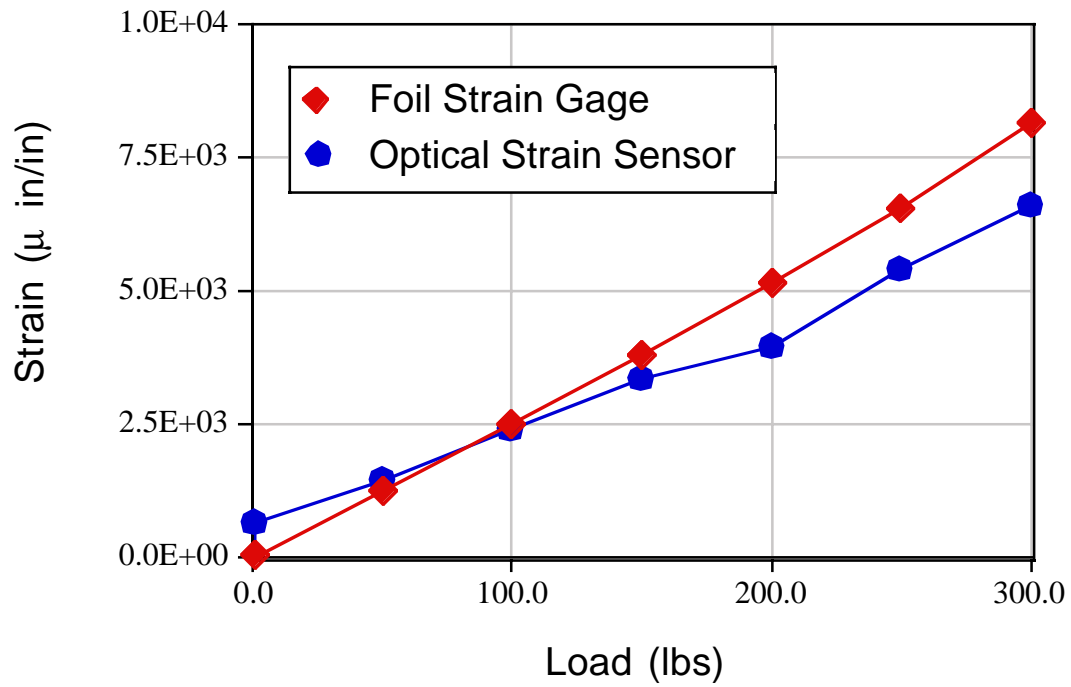


Figure 11. Sample B, comparison of foil strain gage and optical strain sensor data

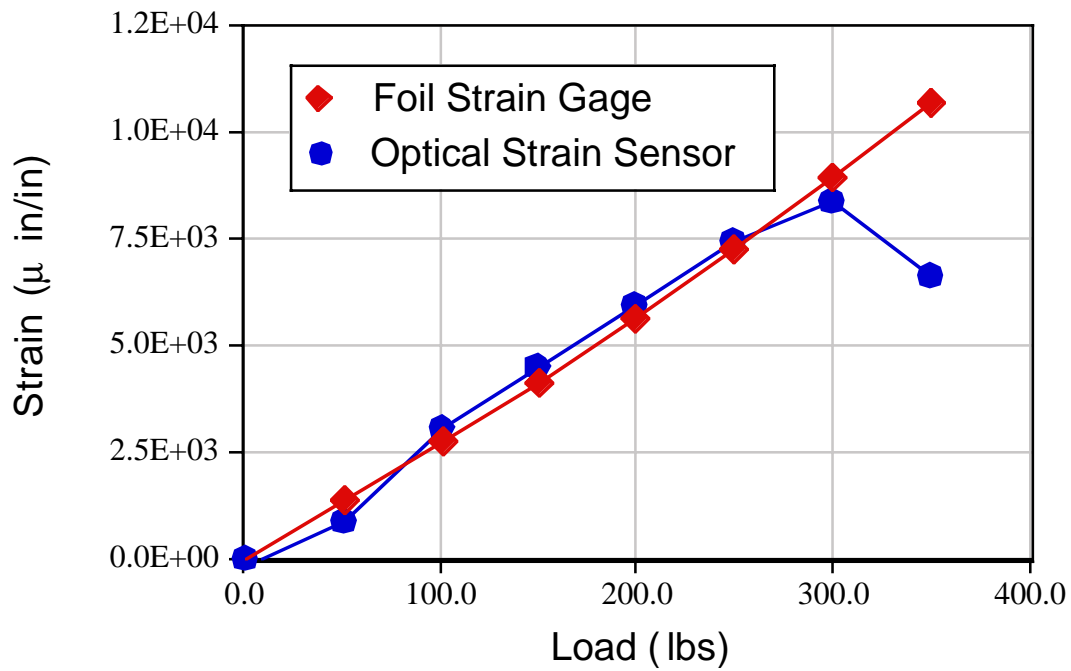


Figure 12. Sample C, comparison of foil strain gage and optical strain sensor data

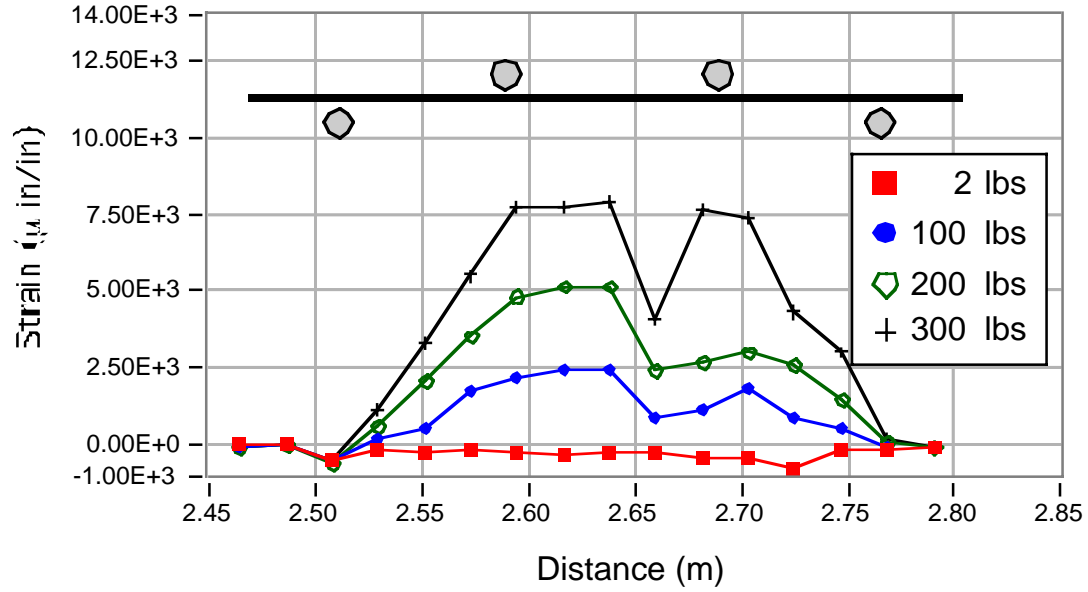


Figure 13. Strain distribution across Sample A for loads of 2, 100, 200, and 300 lbs. A schematic of the sample and loading points is approximately positioned above the strain distribution for reference, based on the strain distribution

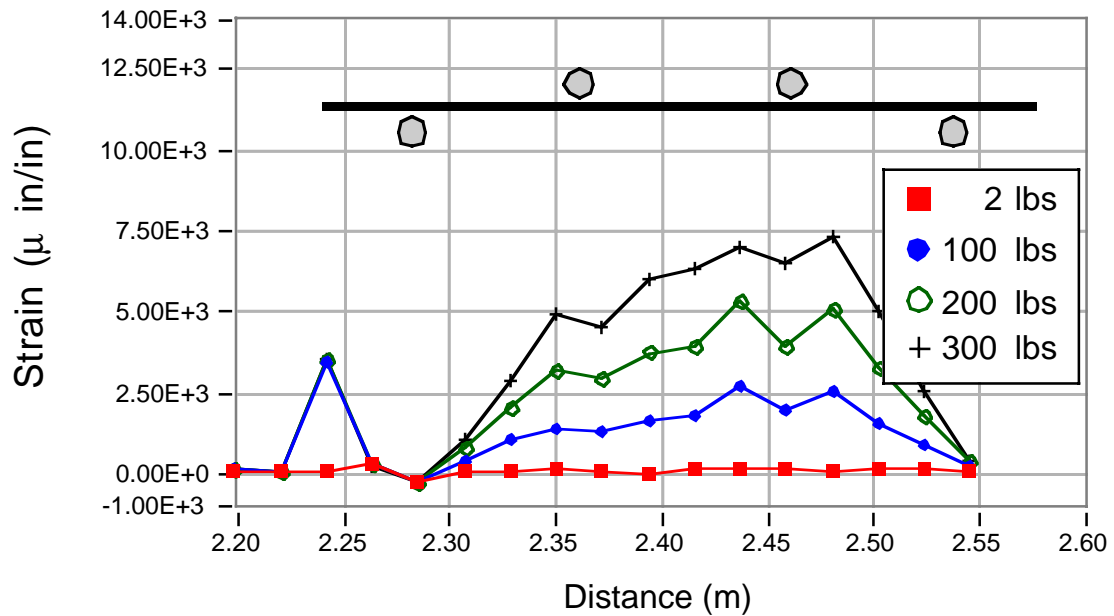


Figure 14. Strain distribution across Sample B for loads of 2, 100, 200, and 300 lbs. A schematic of the sample and loading points is approximately positioned above the strain distribution for reference, based on the strain distribution

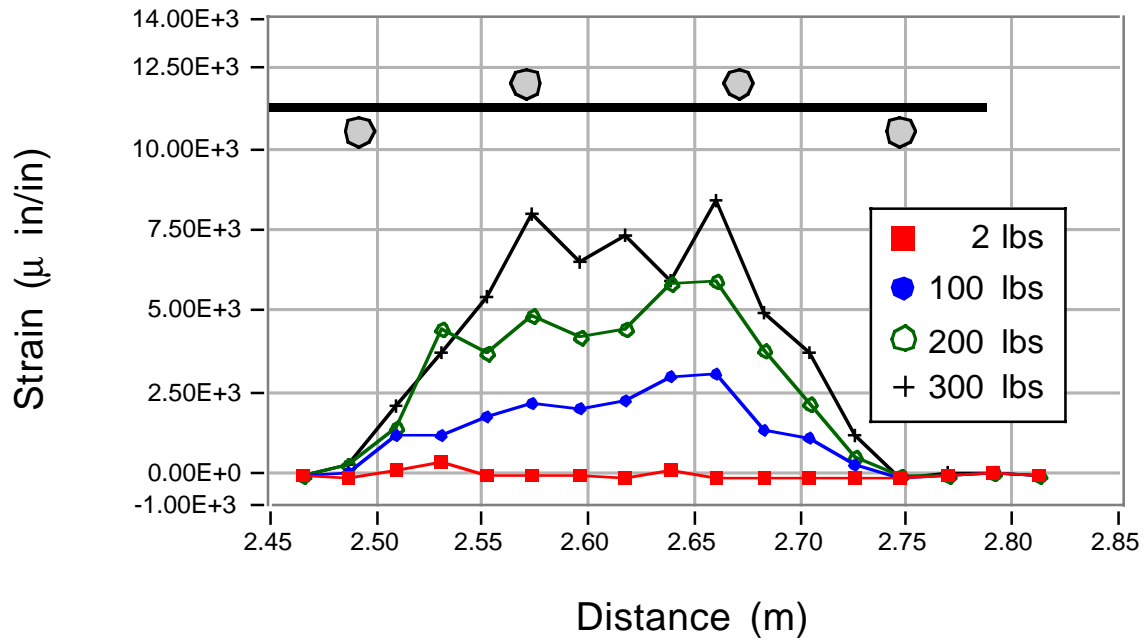


Figure 15. Strain distribution across Sample C for loads of 2, 100, 200, and 300 lbs. A schematic of the sample and loading points is approximately positioned above the strain distribution for reference, based on the strain distribution

REPORT DOCUMENTATION PAGE			Form Approved OMB No. 0704-0188	
Public reporting burden for this collection of information is estimated to average 1 hour per response, including the time for reviewing instructions, searching existing data sources, gathering and maintaining the data needed, and completing and reviewing the collection of information. Send comments regarding this burden estimate or any other aspect of this collection of information, including suggestions for reducing this burden, to Washington Headquarters Services, Directorate for Information Operations and Reports, 1215 Jefferson Davis Highway, Suite 1204, Arlington, VA 22202-4302, and to the Office of Management and Budget, Paperwork Reduction Project (0704-0188), Washington, DC 20503.				
1. AGENCY USE ONLY (Leave blank)		2. REPORT DATE August 2001		3. REPORT TYPE AND DATES COVERED Technical Memorandum
4. TITLE AND SUBTITLE Application of a Fiber Optic Distributed Strain Sensor System to Woven E-Glass Composite			5. FUNDING NUMBERS WU 706-61-11-01	
6. AUTHOR(S) Robert F. Anastasi and Craig Lopatin				
7. PERFORMING ORGANIZATION NAME(S) AND ADDRESS(ES) NASA Langley Research Center Hampton, VA 23681-2199			8. PERFORMING ORGANIZATION REPORT NUMBER L-18100	
9. SPONSORING/MONITORING AGENCY NAME(S) AND ADDRESS(ES) National Aeronautics and Space Administration Washington, DC 20546-0001 and U.S. Army Research Laboratory Adelphi, MD 20783-1145			10. SPONSORING/MONITORING AGENCY REPORT NUMBER NASA/TM-2001-211051 ARL-TR-2435	
11. SUPPLEMENTARY NOTES Anastasi: Vehicle Technology Directorate, ARL, Langley Research Center, Hampton, VA; Lopatin: National Research Council, Langley Research Center, Hampton, VA.				
12a. DISTRIBUTION/AVAILABILITY STATEMENT Unclassified-Unlimited Subject Category 31 Distribution: Standard Availability: NASA CASI (301) 621-0390			12b. DISTRIBUTION CODE	
13. ABSTRACT (Maximum 200 words) A distributed strain sensing system utilizing a series of identically written Bragg gratings along an optical fiber is examined for potential application to Composite Armored Vehicle health monitoring. A vacuum assisted resin transfer molding process was used to fabricate a woven fabric E-glass/composite panel with an embedded fiber optic strain sensor. Test samples machined from the panel were mechanically tested in 4-point bending. Experimental results are presented that show the mechanical strain from foil strain gages comparing well to optical strain from the embedded sensors. Also, it was found that the distributed strain along the sample length was consistent with the loading configuration.				
14. SUBJECT TERMS Fiber Optics Sensor; Bragg grating; Strain; Composites			15. NUMBER OF PAGES 19	
			16. PRICE CODE	
17. SECURITY CLASSIFICATION OF REPORT Unclassified	18. SECURITY CLASSIFICATION OF THIS PAGE Unclassified	19. SECURITY CLASSIFICATION OF ABSTRACT Unclassified	20. LIMITATION OF ABSTRACT UL	